REVIEW

**ADVANCED
PHOTONICS
RESEARCH**
Open Access

www.adpr-journal.com

Super-Resolution Imaging and Optomechanical Manipulation Using Optical Nanojet for Nondestructive Single-Cell Research

Alina Karabchevsky,* Tal Elbaz, Aviad Katiyi, Ofer Prager, and Alon Friedman

Advanced photonic tools may enable researchers and clinicians to visualize, track, control, and manipulate biological processes at the single-cell level in space and time. Biological systems are complex and highly organized on both spatial and temporal levels. If biological entities are to be studied, perturbed, engineered, or healed, key-players in such systems must be visualized and it is required to track, control, and manipulate them precisely and selectively. To achieve this goal, the engineering of nondestructive tools allows to interrogate and manipulate the function of proteins, pathways, and cells for physicians, enabling the design of "smart materials" that can direct and respond to biological processes. Among the potentially exploitable nondestructive tools, light-based actuation is particularly desirable. It enables high spatial and temporal resolution, dosage control, minimal disturbance to biological systems, and deep tissue penetration. Herein, existing approaches toward the engineering of light-activated tools for the interrogation and manipulation of single-cell processes are overviewed, and the types of studies and types of functions that can be controlled by light are listed. Timely applications, such as studies of inflammation and crossing brain barrier systems—via super-resolution imaging and optomechanical manipulation—are two representative examples of emerging applications so far never addressed.

1. Introduction

Existing methodologies in the engineering of light-activated tools limit the types of studies and functions that can be controlled by light for the interrogation and manipulation of single-cell processes.

Understanding biological systems such as the origin, evolution, development, and prognosis[1] of diseases is dictated by processes within a single cell; therefore, research at the single-cell level is an important field in molecular biology and medicine. The first and most used approach used is to closely view a sample through the magnification of a lens, using visible light (**Figure 1**a). The wave nature of light limits the 3D resolution in classic optical microscopy. Ernst Abbe described the resolution limit of an optical microscope.[2] Using wave optics, Abbe showed that the limit in the ability of a conventional optical microscope to resolve an object is $dx = k\lambda/\mathrm{NA}$, where d is the distance between two point sources, and NA is the numerical aperture, $\mathrm{NA} = n\sin\theta$, where θ is the half angle of the light cone that can enter the lens (objective) from a point source, and n is the refractive index of the object space. Depending on the definition, the coefficient k is in the range of 0.473−0.61 and the resolution is in the range of 200−500 nm. However, optical microscopes are unable to reach a theoretical optical resolution due to aberrations and imperfections in classical optics and also suffer from low-contrast images captured from cells.[3–5]

The second approach, developed in the 20th century and widely used for the studies of dynamics and localization of intra- and extracellular components in cells, utilizes organic fluorescent dyes.[2,6–8] However, utilizing naturally light-responsive fluorophores to engineer light-mediated control over a diversity of proteins or functions can be difficult or impossible, highlighting the most significant drawback of this approach, which is its lack of generality and its inability of sustaining long-lasting fluorescence due to fast photobleaching. Because of light stability (photostability), fluorescent semiconductor quantum dots (QDs) have been proposed as an alternative to organic fluorescent optical probes[9]; however, they cannot be used in live cells due to their cytotoxicity and strong blinking.

The third approach was developed in the early 21st century and provides super-resolution imaging in live cells.[10] The most common method for super-resolution techniques which involves fluorescence is stimulated emission depletion (STED)
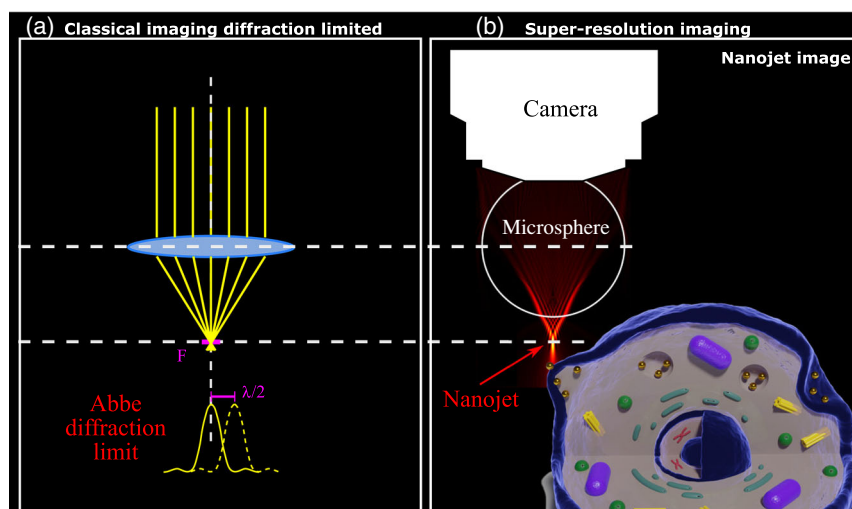
A. Karabchevsky, T. Elbaz, A. Katiyi
School of Electrical and Computer Engineering
Electro-Optics and Photonics Engineering Department
Ben-Gurion University of the Negev
Beer-Sheva 8 410 501, Israel
E-mail: alinak@bgu.ac.il

O. Prager, A. Friedman
Faculty of Health Science
Ben-Gurion University of the Negev
Beer-Sheva 8 410 501, Israel

Figure 1. Concept of classical imaging as compared with super-resolution imaging. a) Classical imaging microscopy with a conventional lens where the system is limited by Abbe diffraction limit as illustrated below. b) Illustration of super-resolution imaging by microsphere with nanojet.

microscopy.[11,12] This method is based on selectively deactivating the fluorescence with a doughnut-shaped beam and confining it in a smaller point. It can achieve 50−60 nm lateral resolution.[13] Another method is single-molecule localization microscopy (SMLM)[14,15] which is based on localizing an individual fluorescent molecule. SMLM can achieve high spatial resolution, typically ≈20−50 nm. This method is used in photo-activated localization microscopy (PALM)[16] and stochastic optical reconstruction microscopy (STORM).[17] In addition, super-resolution can be achieved in a label-free manner. One method for high resolution is coherent anti-Stokes Raman scattering (CARS) microscopy,[18] which is a nonlinear optical version of Raman scattering. The elastic scattering which appears in Raman scattering is canceled by illumination with pump and Stokes beams, forcing only inelastic scattering (anti-Stokes) to occur. This method provides high resolution and fast imaging. Another method is based on phase difference and is called quantitative phase imaging (QPI).[19,20] QPI is a very powerful tool for free-label imaging because it combines microscopy, holography, and light scattering techniques. It can be used for imaging completely transparent structures. Substantial drawbacks of this approach are 1) that the smallest feature it can detect is in the level of noise that stems from the fluctuation in the data and 2) incompatibility with conventional camera technologies such as CMOS cameras. In addition, this method is inherently irreversibly destructive and, once applied, the protein or molecule cannot revert to its original state. Thus, this technology is limited to a one-time-only usage that imposes a substantial restriction on the types of studies and applications that can be advanced with this methodology.

The fourth approach was developed for 3D optical manipulation of microparticles, cells, and biomolecules in a noncontact and noninvasive manner, by the use of optical tweezers.[21,22] Despite being a widely used optical manipulation technique, it is limited in precise manipulation in biological applications because of its bulky lens system and limited penetration depth. As the diameter of biomolecules is in the range of 1−10 nm (small molecules such as IL-1β are in the range of 4−7 nm), the optical tweezer cannot directly manipulate them due to the diffraction limit of light. Emerging near-field methods of plasmonic tweezers and photonic crystal resonators can overcome these limitations; however, their heating effect may damage biological specimens.[23] In this review, we summarize the development of advanced photonic tools for biological research at a scale of single-cell investigation. The article is structured as follows. Section 2 is focused on the super-resolution configurations that allow visualizing tiny changes in a cell. Section 3 describes the fundamental formation of optical forces. Section 4 elaborates on the utilization of gold nanoparticles (NPs) for single-cell investigation. Section 5 is focused on the computational methods to design the optical system and analyze its output. Section 6 shows two representative examples of emerging applications.

2. Super-Resolution Imaging

To trace and view the biological processes such as endocytosis and exocytosis of NPs encapsulated by small molecules such as IL-1β ligands by macrophage cells or others, one can utilize the photonic nanojet (PNJ) effect (Figure 1b). PNJ is one of the approaches developed to break the postulate dictated by Abbe in classical optics (Figure 1a). One such approach is the PNJ effect.[24−26]

A PNJ is a narrow light beam situated near the shadow-side surface of an illuminated dielectric microsphere, whose diameter is comparable with one or a few wavelengths of the light source.[26] The nanojet exhibits: 1) high intensity (up to ×100 of the incident power density); 2) subdiffraction beamwidth; 3) several wavelengths' long reach. In Lee et al. observed that self-assembled nano- or microlenses can resolve features beyond the diffraction limit using an ordinary white-light microscope.[27] Wang et al. reported that dielectric microspheres illuminated with white light and combined with a standard microscope

are capable of reaching resolution features as small as 50 nm resolution integrated with a standard microscope.[28] Such a remote-mode microsphere nanoimaging system can allow a working distance larger than the wavelength of the light source. While these studies illustrate the feasibility of breaking the fundamental Abbe limit to achieving super-resolution imaging, the technologies used have a significant drawback: The described auxiliary structures such as self-assembled nano- or microlenses or dielectric microspheres operate in air, which limit the general applicability of these technologies to biological applications. **Figure 2** shows the super-resolution imaging setups and the imaging outcomes for visualization at a single-cell level. The common method utilizes a microsphere for super-resolution, as shown in Figure 2A. This method uses a microsphere as a magnifier and can achieve a super-resolution of 680 nm.[29] Another method for biological application is using biocell magnifiers, as shown in Figure 2B. These biomagnifiers enable a resolution of up to 100 nm and prevent mechanical and photothermal damage to biospecimens.[30]

Magnifiers can be engineered from biocompatible $BaTiO_3$, whereas the auxiliary structure is of a cylindrical shape. **Figure 3** shows photonic jet formation via 12 μm $BaTiO_3$ microcylinder with refractive index $n_{cylinder} = 2.4 - 2.5$ in water (refractive index $n_{water} = 1.33$) for two for 520 and 637 nm,

respectively. The refractive index contrast between water and $BaTiO_3$ is high enough and is therefore suitable for biological environments.[31]

Table 1 shows calculated results of key parameters of a photonic jet formation via an illuminated 12 μm $BaTiO_3$ microcylinder auxiliary structure in water. The full width at half maximum (FWHM) values demonstrate super-resolution values beyond the diffraction limit, which is half of the wavelength. The focal point of maximum intensity is measured from the microcylinder, is formed at the near field, and enables the effect of narrowing of the photonic jet that exists only near the particle surface.[32]
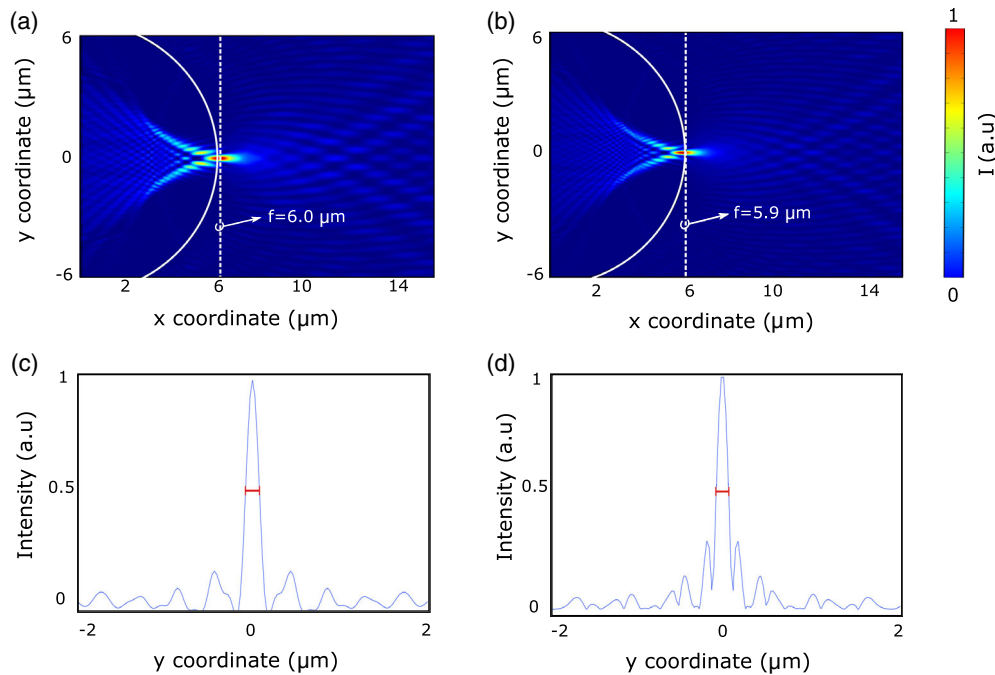
3. Optical Forces

3.1. Fundamentals of Optical Forces

Shortly after the laser was invented, Ashkin proposed and demonstrated[33] that the incident laser beam can be implemented to trap and manipulate dielectric particles and even cells.

The optical force on the mesoscale particles of micro- or nanoscale is a consequence of the conservation law of electromagnetic wave momentum. At these sizes, the particle does not correspond to the gravitational force but to the radiation pressure and the Lorentz force. Theoretical modeling of optical forces
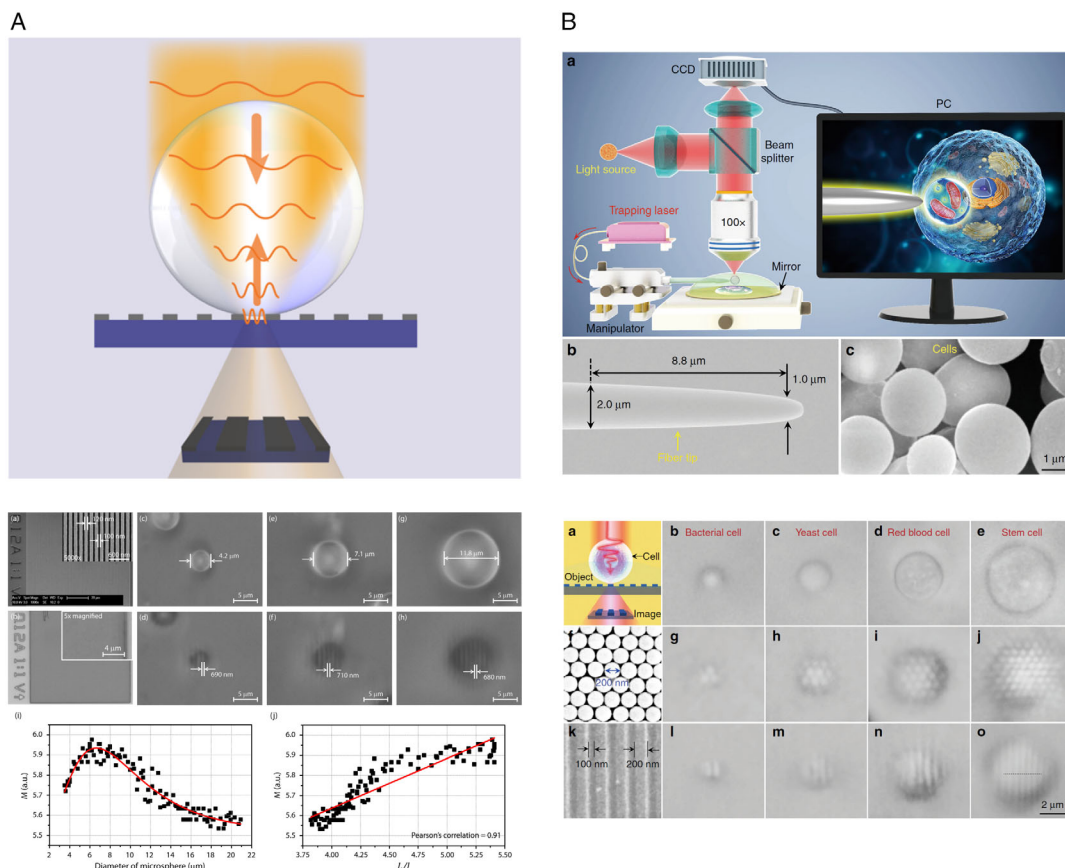
Figure 2. Super-resolution imaging. A) Magnification by a dielectric microsphere. Reproduced with permission.[29] 2016, ACS Publications B) Super-resolution by biomagnifiers. Top line shows schematic of the experimental setup used for attaching the biospecimens to the probe fiber. Bottom line shows different resolutions of different objects with a variety of biomagnifiers. Reproduced with permission.[30] 2019, Nature Publishing Group.

**ADVANCED
SCIENCE NEWS**

www.advancedsciencenews.com

**ADVANCED
PHOTONICS
RESEARCH**
Open Access

www.adpr-journal.com

Figure 3. Calculated photonic jet out of BaTiO$_3$ microcylinder with diameter of 12 μm in water medium illuminated at wavelength of a) 520 nm and b) 637 nm. Normalized distribution of intensity for wavelength of c) 520 nm and d) 637 nm.

Table 1. Key parameters of a photonic jet generated via 12 μm BaTiO$_3$ microcylinder in water for two different wavelengths in visible light.

Wavelength [nm]	Focal length [μm]	Max intensity [W m^{-2}]	FWHM [nm]	Longitudinal length [μm]
520	5.9	68.2×10^{-3}	0.30λ	1.3
637	6.0	51.4×10^{-3}	0.22λ	1.6

was discussed by Debye,[34,35] showing that the force applied on a sphere can be described in terms of extinction and scattering cross sections as a function of microsphere dimensions with respect to the beam wavelength. Ashkin set the foundations of optical trapping of micrometer-sized particles, resulting from the radiation pressure from an intense, coherent laser.[36,37] For this discovery, he was awarded the Nobel prize in 2018.[38] The radiation pressure, expressed by the momentum carried by a single photon p, has two different approaches of calculation, known as the Abraham–Minkowski controversy.[34]

$$p_{\text{Min}} = \hbar k = \frac{n\hbar\omega}{c} \tag{1}$$

or

$$p_{\text{Abr}} = mv = \frac{\hbar\omega}{nc} \tag{2}$$

where $\hbar$ is the reduced Planck's constant, ω is the angular frequency of the light, c is the speed of light in a vacuum, and n is the refractive index of the medium. Barnett suggested that p_{Min} describes the canonical momentum, while p_{Abr} describes the

kinetic momentum. When considering Minkowski's force theory and Abraham's force theory as time-averaged forces, the stress tensor coincides for both. In the case of a Rayleigh particle, when the object is much smaller than the wavelength, it behaves like an electric dipole.[36,39] The Lorenz–Mie theory, among others, is an analytical method designed for plane-wave scattering by a spherical particle. Barton and co-workers added corrections to the fundamental Gaussian beam, enabling the derivation of the incident and scattered fields from a sphere.[40] In this way, the force can be calculated by means of integration of the Maxwell stress tensor **T**, which is the time-averaged optical force acting on a particle over a closed surface ∂V surrounding the particle.[30,41]

$$\langle \mathbf{F} \rangle = \int_{\partial V} \langle \mathbf{T}(\mathbf{r}, t) \rangle \cdot n(\mathbf{r}) \mathrm{d}A \tag{3}$$

where **T** is the time-averaged Maxwell stress tensor and n is the normal to the surface.

We generally refer to the particle being moved around by this force as the "probe" or "target," bearing an arbitrary rigid shape and size. However, for numerical simulations, this method of obtaining optical forces is computationally intensive. For instance, to obtain the full force field over a 2D space, we would need to place the probe particle in one specific point in space, evaluate the electromagnetic field in this configuration, and then integrate over the surface around the probe to obtain the forces, repeating the process over a 2D grid of points. In addition, the simulation in this method is to be conducted using the full 3D geometry.

Assuming that our probe is within the Rayleigh regime (i.e., the incident wavelength is much larger than probe dimensions),

we can assume that the optical force acting on the target can be described using Taylor's expansion. Physically, this would imply that the probe is approximated to only have electric and magnetic dipole moments. The optical force equation becomes[41,42]

$$\langle \mathbf{F} \rangle = \frac{1}{2} \text{Re}[(\nabla \mathbf{E}_i^*) \cdot \mathbf{p}] + \frac{1}{2} \text{Re}[(\nabla \mathbf{B}_i^*) \cdot \mathbf{m}] \\ - \frac{k^4}{12\pi\varepsilon_0 c} \text{Re}[\mathbf{p} \times m^*] + \ldots \tag{4}$$

We deal with only the first term of Equation (4), which corresponds to the force if the probe was assumed to be only an electric dipole. The second term (the force if we were also to consider a magnetic dipole term in the Taylor series expansion), the third term (the force due to the interaction of the two dipoles), as well as all higher-order terms are negligible and can be ignored. This approximation also greatly simplifies numerical simulations, as we have to obtain only the electromagnetic fields on one plane and the domain can also be simplified into 2D geometry (whenever applicable).

The first term of Equation (4) can be written in the following form.

$$\langle \mathbf{F} \rangle = \frac{\alpha'}{4} \nabla E_0^2 + \frac{\alpha''}{2} E_0^2 \nabla \phi \tag{5}$$

where α is the probe complex polarizability. For a spherical particle, this is given by[43]

$$\alpha = 4\pi r^3 \varepsilon_0 \frac{\varepsilon_p - \varepsilon_a}{\varepsilon_p + 2\varepsilon_a} \tag{6}$$

We note that the value of the polarizability is dependent on the difference of the dielectric permittivities of both the probe particle ε_p and the surrounding material ε_a. As described in **Figure 4**, the first term in Equation (5) is the "gradient force," which arises from field inhomogeneities and is proportional to the dispersive interaction of the induced atomic dipole with the intensity gradient of the light field,[44] whereas the second term is the "scattering force," which can be regarded as a consequence of momentum transfer from the radiation field to the particle, proportional to the dissipative (imaginary) part of the complex polarizability.[41] Note that the phase ϕ can be written in terms of the **k** vector such that $\nabla\phi = \mathbf{k}$.

For certain biological applications, such as label-free manipulation of cells, the polarization α is very low due to the low permittivity contrast of the probe and the environment; hence, a high-power and highly focused incident field is required for this application. This then raises the problem of heating. In addition to the potential for altering or damaging the biological samples, heating can also influence the motion of the targets due to thermophoretic effects.[45] One method of solving the contrast problem is to add gold NPs in the cells to serve as "handles" which can influence the movement of the entire system. As a solution, one can use the photonic hook (PH) to move cells in their liquid background,[46] as detailed in the following subsection.

3.2. Optomechanical Manipulation: Moving Objects in Inter- and Intracellular Media

To move objects in inter- and intracellular media by the use of light, one needs to create an optical force (see preceding section). Based on the properties of the electromagnetic field, optical forces can be classified into two main categories, namely, scattering and gradient forces. The capability of light to exert forces on particles, a phenomenon known as radiation pressure, is well known and extensively documented in the literature. Historically, demonstrations of radiation pressure showed that this force is very small, but with the invention of the highly directed and focused laser beams, control over the position of small objects can be realized. The act of moving objects with the help of electromagnetic forces is termed "optical tweezers." Optical tweezers have found applications in biology and nanotechnology; however, they come with several limitations. Highly focused laser beams require expensive, complicated, and bulky lens set-ups. Multiple traps can be formed through different methods that require increased laser power input, etc.

Producing mechanical action on particles through electromagnetic radiation was first hypothesized from the observation that the direction of a comet tail points away from the sun. Kepler suggested that this phenomenon is a result of radiation pressure, and Maxwell[47] later showed that momentum transfer from the electromagnetic (EM) field to an object results in this radiation pressure. Specifically, he showed that the force on an object absorbing P watts of light is given by $F = P/c$, whereas for a perfectly reflecting object, this force is $F = 2P/c$.
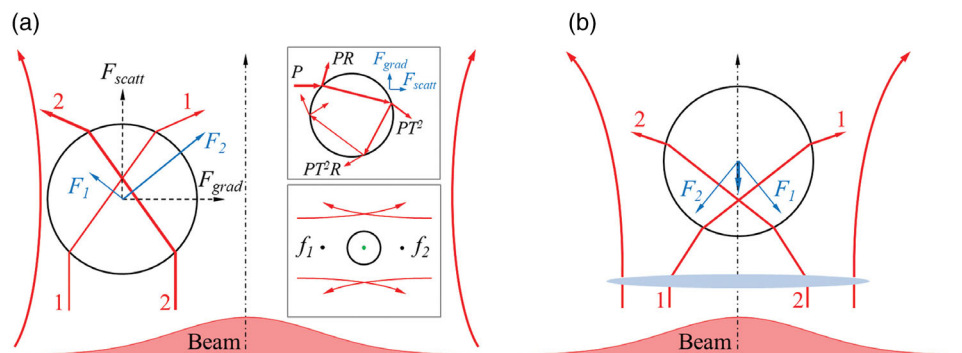
Figure 4. Optical forces acting on a dielectric microsphere illuminated by a Gaussian beam. a) Total forces resulting from scattering force F_{scatt} and gradient force F_{grad} and b) net forces resulting from focused rays. Reproduced with permission.[36] 2018, Wiley-VCH.

Lebedev[48] and Nichols[49] independently showed this effect experimentally for macroscopic objects in 1901 and 1903, respectively. In addition, Lebedev also studied optical forces on gases.[50] By manipulating the field, Ashkin[51,52] showed experimentally that it is possible to trap particles at the field focal point, showing that control of the field can be used to reposition objects and even to move particles opposite to the direction of the incident field.[53–55]

3.3. Photonic Jet and PH Formation

The conventional approach for generating an optical force utilizes high-magnification objectives for focusing the laser beam, as shown in **Figure 5**A, for instance, for levitating particles,[56] as shown in Figure 5B. While the traditional microscope-based trap has found applications in a wide variety of disciplines, such as biophysical research, the light-based approach is diffraction limited. Thus, achieving manipulation on the nanoscale requires auxiliary structures that generate tightly confined electric fields.

The PNJs are nonevanescent and low-divergence localized spots with high intensity[57] that are observed on the shadow side of the surface of the auxiliary structure (spherical or square,[58] cylindrical,[59] or other shapes[60,61]) when illuminated by a plane wave[62] or pulsed illumination.[60] The PNJ is generated at the near field due to a wavefront deformation resulting from interactions of the low-absorbing microelement boundary and the illuminating field. According to Mie's theory, the optical fields inside and outside the dielectric microelement are subject to the light wave, focusing it and acting as a refractive microlens due to the curvature of the particle surface. It has negligible aberration and high NA when the refractive index contrast between the microsphere and its surrounding medium is about 1.5.[30,63,64] The PNJs are characterized by FWHM, capable of going beyond the diffraction limit.[65] Due to their unique properties, they can be utilized for super-resolution imaging, photolithography at nanoscale, and biological applications, using NPs.[64] The key parameters of PNJs are focal distance, longitudinal size, maximum intensity, and a lateral FWHM (see Table 1), which depend strongly on the refractive index contrast and auxiliary structure dimensions.[64,66]

The actual generation of PNJs is usually realized with a plane wave incident on spherical or cylindrical NPs,[59,67,68] but PNJs are also generated from nonspherical particle cross sections such as in other studies.[46,60,61,65,69,70] In addition, photonic jets have been previously used for optical manipulation applications, the first of which was done by Cui et al.,[71] where they obtained the forces on a metallic NP immersed in the PNJ field. This way, they can be used for manipulation and detection of biological targets.[72]

PNJs, discussed earlier, can also be generated using other symmetric structures. In the context of optical manipulation at a single-cell level, the continuous wave (CW) field-based illumination causes heating to the system, which can be potentially destructive. To overcome the destructive operation of CWs, an alternative approach of pulsed laser-generated input field[60,73] was proposed. It was shown[60] that this approach also increases the optical force performance, which has been demonstrated experimentally with femtosecond lasers while trapping latex NPs.[74] Because of its conservative character, the optical force can be derived from potential energy, the minima of which can be used for light-activated motion. Optical forces are usually generated using spherical structures subjected to the illumination of a plane CW. When optical forces in the form of PNJs are applied on a metallic NP, the forces acting on this NP are the result of the momentum exchange.[71]

Worth noting is that these previous works are primarily focused on trapping the particles along some axis of symmetry. Curved photonic jets, named PHs, can be used for creating forces that move an object in inter- or intracellular media in a curved trajectory. These PHs are made possible using
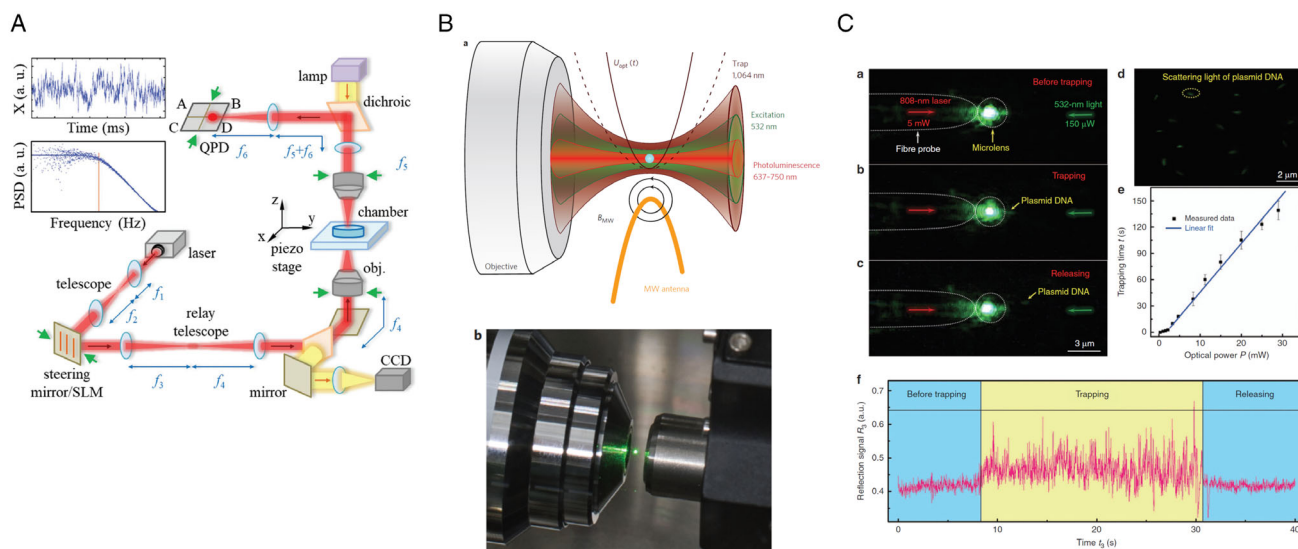
Figure 5. Examples of optical forces exerted on a cell or particle. A) Conventional optical tweezer system. Reproduced with permission.[36] 2018, Wiley-VCH. B) a) A hybrid nano-optomechanical system and b) a levitated nanodiamond. Reproduced with permission.[56] 2015, Nature Publishing Group. C) Optical tweezers for biosamples by a nanojet with a probe fiber. Reproduced with permission.[129] 2016, Nature Publishing Group.

asymmetric particles.[75,76] By breaking the symmetry of an auxiliary object, the generated structured light beams become curved. This effect is known as a curved photonic jet or PH[69,77–79] and has unique properties of a tilt angle depending on deformation.[59] Specifically, PH experiences both lateral size and a radius of curvature as a fraction of the incident wavelength.[79] The distinctive features of the PH are that the transverse size and curvature radius of the beam are a fraction of the incident wavelength and that the side lobes differ from the shape of the main beam and so do not bend. The generation of well-studied curved airy beams usually requires expensive and complicated optical elements with a cubic phase, which makes optical elements incompatible with optical systems. The geometries of PH systems are shown in **Figure 6**. The simple method for breaking the symmetry that will create a PH is by breaking the symmetry of illumination, as shown in Figure 6A. This can be done via blocking part of the input light of an auxiliary structure, as studied by Minin et al.[59] By varying the thickness of the blocked beam, for instance with a mask, one can tune the angle of the hook. Another method is to break the symmetry of the focusing object itself. By locally changing the refractive index of the cylinder, one can break the system symmetry,[80] as shown in Figure 6B. Another method is by fabricating a nonsymmetric structure,[77] as shown in Figure 6C.

Configurations for PHs have been optimized,[75] investigated for optomechanically moving NPs around obstacles,[77] and recently experimentally demonstrated.[59] Previously, PH-based optical manipulation under CW illumination was explored, but the generated force has a small magnitude for realistic applications.[77] As mentioned earlier, one way to mitigate the destructive effect of CW illumination is utilizing a pulsed input field.[60]

Despite rapidly progressing advances in engineering tools activated by light and operating optomechanically in biological media such as optical tweezers, only a small force can be generated, due to fundamental limitations of current methods involving CW light. The approach for engineering light-activated tools is by the generation of optical forces—a class of forces known to experience nondestructive light-activated motion— among them optical tweezers, airy beam, PNJs, and PHs.[75] The first property of interest to us is that the PNJ and PH have enabled the engineering of motion tools for sorting, PNJ surgery, and others, overcoming the obstacles of light scattering and absorption.[81] The second property of interest to us is that optical forces provide a fundamental property of light to develop a practical platform to study processes within the cell, overcoming the need for fluorescent staining.[82–84] This property allows natural label-free characterization of biological processes. Recent studies illustrate the feasibility of utilizing optical forces for instance: in vesicles (size from tens to thousands of nanometers),[85,86] in manipulating and dragging a selection of liquid domains in lipid bilayers,[87] in trapping viruses (thousands of nanometers),[88] and in trapping,[21,22,89] sorting,[90] and isolation[91] of bacteria and living cells. However, the technologies used have one significant drawback, which is the small optical force able to attract or repel an object, thereby rendering them not feasible for actual applications in cell biology research. The scattering force is directly associated with the wavevector of light and is interpreted as the momentum interchange between light and objects, when the propagation path is altered owing to discontinuities in the refraction index. The gradient force essentially refers to the gradient of the field energy intensity, which plays an important role in forming traps by overcoming the scattering force.

4. Plasmonic Gold NPs for Local Treatment

Plasmonic NPs are widely used in biological research for drug delivery, temperature-assisted treatment, and other procedures.
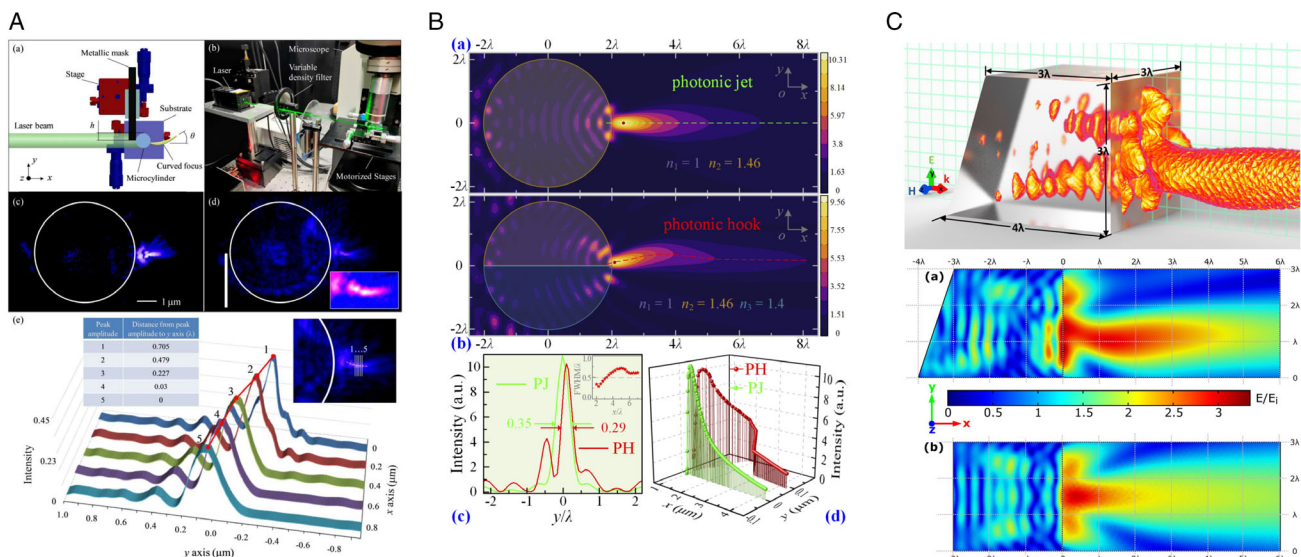
Figure 6. Configurations for PH A) A dielectric microcylinder with cover by a metallic mask. Reproduced with permission.[59] 2020, Optical Society of America. B) Asymmetric microcylinder made by two different materials. Reproduced with permission.[80] 2019, Optical Society of America. C) A symmetric prism. Reproduced with permission.[77] 2018, Nature Publishing Group.

ADVANCED
SCIENCE NEWS
www.advancedsciencenews.com

ADVANCED
PHOTONICS
RESEARCH
Open Access
www.adpr-journal.com
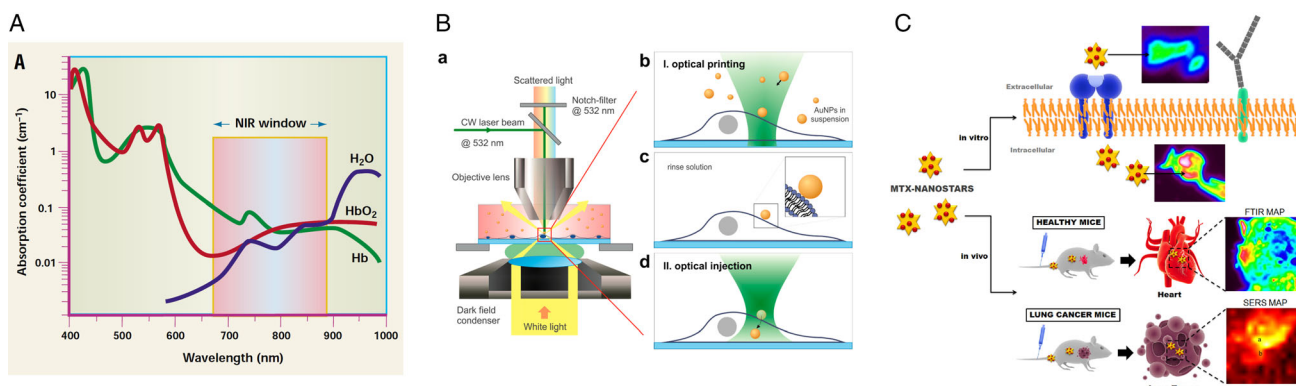
Figure 7. A) Human tissue transmission window in the near-infrared. Reproduced with permission.[94] 2015, ACS Publications. B) Illustration of the optical force system for injecting gold NPs into a living cell. Reproduced with permission.[94] 2015, ACS Publications. C) Gold nanostars for efficient drug delivery and monitoring of cancer cells. Reproduced with permission.[95] 2016, Elsevier.

Due to their highly polarizable conduction of electrons, gold NPs can be used for interaction with the electromagnetic field. In addition, plasmons in gold NPs are excited at $600-900$ nm, allowing deeper penetration, as the cells have low absorption at visible wavelengths[92] as shown in **Figure 7**A. In 1996, the first demonstration used gold NPs to show that insertion of a protein into rat kidney cells.[93] Subsequently, gold NPs were injected into a living cell using a focused laser beam[94] as shown in Figure 7B. Due to the shift in the gold nanoparticle (GNP) plasmon absorption, the change in the placement of the NPs can be verified. The capability of gold NPs to be directed to a specific location can be utilized for NP-targeted drug delivery. As it is relatively straightforward to attach to the gold via a thiolated tail and other methods, it is possible to efficiently control the drug concentration with gold NPs by laser radiation,[95] as shown in Figure 7C. Plasmonic gold NPs can also be used for imaging. By changing the particle shape, the imaging quality can be improved. For example, utilizing the Purcell effect, nanoantenna, and surface plasmon resonance (SPR) effect, gold nanorods can be used for plasmon-enhanced fluorescence (PEF), for weak fluorescence emission, and even for single-molecule detection, with an enhancement factor of up to 1100.[96] **Table 2** shows widely used plasmonic NPs for optomechanical manipulation such as nanospheres, nanostars, and nanorods. Spherical geometry of NPs is used for drug delivery based on membrane perforation, with typical localized surface plasmon excitation at visible wavelengths.[69] However, spherical particles made of Mxene, such as in the study by Spector et al.,[60] are capable of exciting surface plasmons at longer wavelengths in near infrared. Nanostars are useful for imaging applications due to multiple hot spots,[95] whereas nanorods are capable of exciting localized surface plasmon resonance (LSPR) along the longitudinal and transverse directions, as in other studies.[96–99]

5. Computational Approaches

To design an optical system for super-resolution imaging or opto-mechanical manipulation, but also to be able to analyze the obtained experimental results, one may use numerical approaches alongside analytical methods.[40,100] By dividing the structures into small subdomains, numerical methods can efficiently handle complex geometries.[100] Popular and efficient computational approaches used for nano-optics and near-field optics include the finite-element method (FEM), the finite-difference time-domain (FDTD) technique, and the finite integral technique (FIT).[60,100,101] The FDTD, a commonly used numerical modeling tool, is based on an algorithm for discretization of the selected computational domain by proposing a spatial rectangular grid, according to Yee's algorithm.[102,103] Both electric field $\vec{E}$ and magnetic field $\vec{H}$ components are used in a 3D space to numerically solve Maxwell's equations. This is a direct space time-domain method used for solving electromagnetic problems such as pulsed beam illumination and spectroscopic studies. It solves both electric and magnetic fields using the coupled Maxwell's curl equations by iteration over time. When considering a 2D case for the transverse-electric mode TE_z mode, for example, involving only E_x, E_y, and H_z, the set of time-dependent Maxwell's equations will be[102,104]

$$\frac{\partial E_x}{\partial t} = \frac{1}{\varepsilon}\left[\frac{\partial H_z}{\partial y} - \left(J_{source_x} + \sigma E_x\right)\right] \tag{7}$$

$$\frac{\partial E_y}{\partial t} = \frac{1}{\varepsilon}\left[-\frac{\partial H_z}{\partial x} - \left(J_{source_y} + \sigma E_y\right)\right] \tag{8}$$

Table 2. Widely used NPs for optomechanical manipulation.

Shape	Size, [nm]	Application	Wavelength, [nm]	Ref.
Spheres	$5-150$	Cellular medium, drug delivery, Optical injection, membrane perforation PH, photonic jet, LSPR	$520-6\,501\,550$	[60,69]
Nanostars	$30-40$	Drug delivery and enhanced imaging	786	[95]
Nanorods	58×25	Single-molecule enhanced fluorescence	650	[96]

$$\frac{\partial H_z}{\partial t} = \frac{1}{\mu}\left[\frac{\partial E_x}{\partial y} - \frac{\partial E_y}{\partial x} - \left(M_{source_z} + \sigma^* H_z\right)\right] \quad (9)$$

where E_x, E_y is the electric field in x and y directions, respectively, H_z is the magnetic field in z direction, ε is the electrical permittivity, J_{source} is the electrical current density of the source, M_{source} is the equivalent magnetic current density of the source, σ is the electric conductivity, and σ^* is the equivalent magnetic loss. This method is particularly useful for direct calculation of nonlinear response of an electromagnetic system.[104] However, due to its uniform Cartesian grid form for spatial discretization, it limits geometry representation, which results in large memory usage and long computation time. The FEM algorithm is one of the conventional numerical modeling tools for the simulation of near-field problems, as a frequency domain method. It utilizes a mesh made up of tetrahedra, thus combining the advantages of time domain and versatility of spatial discretization procedures and allowing the accurate modeling of complex structures with arbitrarily shaped regions. Furthermore, experimental values of arbitrary dielectric constants for plasmonic micro/nanostructures can be taken into account.[104,105] To solve the wave equation in terms of the electric field which is the curl of Maxwell's equations, the FEM method utilizes a vector testing function v, integrated on the considered volume.[105] For example, for a 2D problem E_x, E_y, and H_z[100]

$$\int_\Omega \left[\nabla\left(\frac{1}{\varepsilon_r}\nabla H_z\right) + \frac{\omega^2}{c^2}H_z\right]v\,d\Omega = 0 \quad (10)$$

where v is the test function defined on a domain Ω. For both methods, FDTD and FEM, the perfectly matching layer (PML) method on the outer surface of the computational domain is utilized to absorb waves incident on the boundary.[102,105] The FIT method covers various electromagnetic problems and can be referred to as a hybrid combination of FDTD and FEM but differs from these methods by discretization of Maxwell's equation in an integral form instead of the differential one. For Cartesian grids, the FIT formulation can be rewritten as a standard FDTD method, and for a triangular grid case, the FIT can be linked with FEM method.[60,100,104]

## 6. What Kinds of Single-Cell Applications are Currently Overlooked?

Here we list two applications in which the described super-resolution and optomechanical approaches are essential.

6.1. Inflammation

The protein cytokine interleukin IL-1β is an inflammation key mediator that is crucial in host–defense responses to infection and injury. IL-1β exacerbates damage during chronic disease and acute tissue injury. However, the lack of engineered user-friendly tools for visualizing, monitoring, and manipulating the protein pathways limits investigation of biological processes at the single-cell level in space and time (**Figure 8**).

Inflammation alarm cytokine IL-1β is considered an "alarm" upstream mediator which initiates and propagates inflammation. IL-1β is secreted mainly by myeloid cells into the environment immediately after the processing of its precursor and accumulates in the affected tissues, where it activates diverse cells which abundantly express the IL-1 signaling receptor type 1 (IL-1R1) and collectively contributes to the inflammatory response. The "alarm" function of IL-1β stems from its ability to induce the expression/secretion of proinflammatory downstream cascades of cytokines/chemokines and also promote cell infiltration through induction of adhesion molecules on endothelial cells and leukocytes. As of now, the majority of IL-1β inhibiting agents, which have also been successfully used clinically in some diseases, neutralize IL-1β already secreted in tissues. These mainly include the IL-1 receptor antagonist (IL-1Ra), which is the physiological inhibitor of IL-1R1 signaling as well as of specific antibodies.[2,106] However, treatment of patients with such agents is usually applied when IL-1β is already present in the arena and the inflammatory response is already full blown. IL-1β is active in minute picogram amounts and binds to IL-1R1 at high affinity. Thus, the binding of IL-1β to about as little as 1% of its surface receptors is sufficient to induce a full cellular response. The development of novel therapeutic drugs based on the inhibition of IL-1β secretion would be possible, thanks to the new light-based technology.

Inflammation alarm cytokine IL-1β is secreted by the "leaderless nonvesicular unconventional protein secretion" process. As the name suggests, this process differs from well-understood conventional protein secretion, and the fine details of this process are yet unclear. Advanced light-based technologies may shed light on this process. Unconventional protein secretion is thought to play a role in numerous diseases.[107] For example, the secretion of the HIV-TAT protein by HIV-infected cells takes place via an unconventional process and is a crucial step in the pathogenesis of AIDS[108]; unconventional secretion of heat shock proteins plays a crucial role in the immunomodulation and proliferation of cancer[109]; and the unconventional secretion of the FGF2 protein has been postulated as a potential therapeutic target for neurodegenerative diseases such as Alzheimer's and Parkinson's disease and multiple sclerosis.[110] Therefore, the development of tools that could start to unravel the mechanisms of unconventional protein secretion could have a great impact in many areas of disease research and could substantially improve our understanding of this intracellular process. IL-1 is an "alarm" cytokine that mediates inflammation, mainly through the induction of a local network of cytokines/mediators. These can serve as potential biomarkers and facilitate cell infiltration into the affected sites through induction of adhesion molecules on endothelial cells and leukocytes.[111] IL-1β and IL-1α are the major agonistic molecules of IL-1 and their proteins are encoded by distinct genes that share only slight sequence homology (20−30%) but considerable 3D similarity, which enables them to bind and signal through a common IL-1 receptor type 1 (IL-1R1). IL-1α and IL-1β are synthesized as precursors of 31 kD that are further processed by distinct proteases to their mature secreted 17 kD forms. IL-1α and IL-1β differ from most other cytokines by lack of a signal sequence, thus not passing through the endoplasmic reticulum Golgi pathway. This raises intriguing mechanistic, functional, and evolutionary questions. In their secreted form,
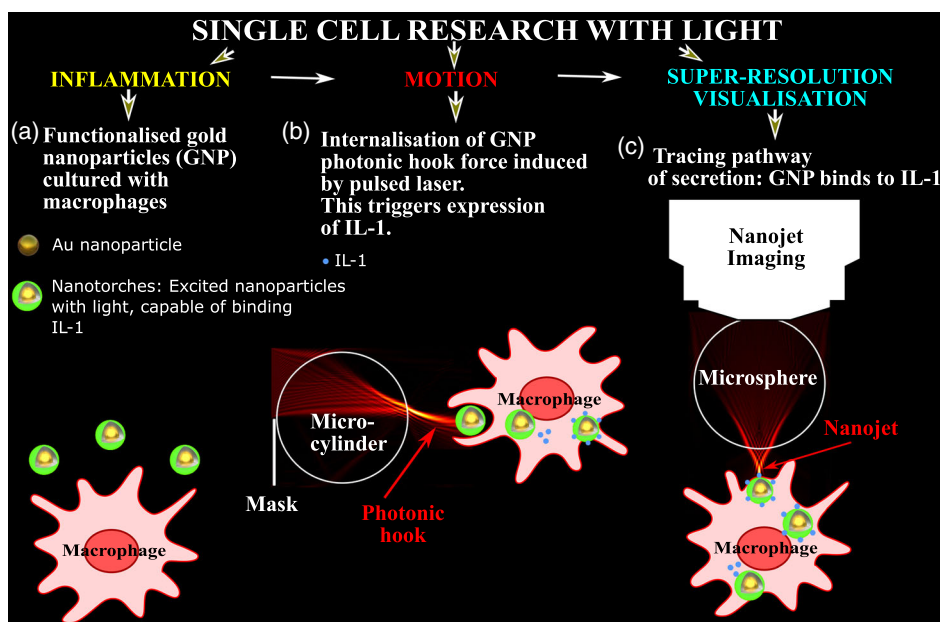
Figure 8. A schematic representation of single-cell process investigation with light a) biological emulator, a cell, b) light-activated tool to initiate internalization and to control the pathways; c) tracking, monitoring, and nanoscale imaging of proteins or pathways. Here, functionalized nanotorch is internalized into the intercellular space with the PH-assisted internalization to trigger the initiation of inflammation cytokine IL-1β, showing calculated repelling curved optical field distribution generated with the microcylinder, generating IL-1 molecules, and IL-1 connected to NPs. The tracking and nanoscale imaging is conducted with the microsphere.

IL-1α and IL-1β induce the same biological functions. However, IL-1α and IL-1β differ in their compartmentalization within the producing cell or the microenvironment. IL-1β is only active in its secreted form and mediates inflammation, which promotes carcinogenesis, tumor invasiveness, and immunosuppression.[2] The mechanism of IL-1β secretion that is active only upon processing and immediate secretion is not completely understood. It has been suggested that the efflux of calcium into the cell activates phosphatidylcholine-specific phospholipase C and calcium-dependent phospholipase A2, which facilitate the secretion of IL-1β together with exocytosis of lysosomal content. The secretion of IL-1β through microvesicle shedding or via an unknown function of the inflammasome has also been suggested.[112] Recent breakthroughs in inflammasome and IL-1 biology have spurred the development of novel anti-IL-1 agents that are being used in clinical trials in patients suffering from diverse diseases with inflammatory manifestations. IL-1Ra is already FDA approved and is safe and efficient in alleviating symptoms of rheumatoid arthritis and other diseases characterized by chronic inflammation. In experimental cancer, IL-Ra attenuates tumor-mediated inflammation and invasiveness. IL-1 is abundant in the tumor microenvironment, where it is secreted by the malignant cells, stromal or inflammatory. In experimental tumor models and cancer patients, enhanced expression of IL-1, especially IL-1β secreted during tumor progression, has been correlated with bad prognosis.[107] Understanding the largely unknown mechanisms of IL-1β secretion will contribute to better understanding of the biology of unconventional protein secretion and finding new approaches for intervention in the inflammatory process in the body in response to infections, injuries, or toxins.

6.1.1. The Relation Between IL-1β Maturation and its Relocation from the Cytosol to the Plasma Membrane

The response to pathogens is orchestrated by the complex interactions and activities of the large number of diverse cell types involved in the immune response. The innate immune response is the first line of defense and occurs soon after pathogen exposure served by phagocytic cells such as macrophages, which conduct this response. Inflammatory macrophages (cells of myeloid lineage) produce an inactive precursor of IL-1β, named pro- IL-1β. Following activation of the cytosolic signaling complex named inflammasome,[113] activated caspase-1 processes the pro-IL-1β to a mature form m-IL-1β in the cytosol, which is then relocated to the plasma membrane and secreted.[114] However, the relationship between cytokine processing and secretion is unresolved. We envision the development of tractable light-activated tools to study cellular systems such as inflammatory macrophages, specifically, to adjust light-activated tools to allow an understanding of the relation between IL-1β maturation and its relocation from the cytosol to the plasma membrane. The experimental strategy may include the creation of a universal platform for super-resolution imaging and tracking and testing this platform in studying the relation between IL-1β maturation and its relocation from the cytosol to the plasma membrane in proinflammatory conditions[115] via expanding light-activated tools.[60,77] The alternative conventional scheme

is a well-studied osmoprotectant glycine to delay caspase-1-dependent macrophage cell rupture and the resultant passive protein release and monitored IL-1β maturation and release upon inflammasome activation in lipopolysaccharide (LPS)-primed macrophages.

Cytokine interleukins (IL-1α and IL-1β) are the major key mediators in inflammatory response and resistance to pathogens of the innate host immune system. Among them, IL-1β is the most powerful cytokine, able to induce inflammatory responses in virtually all tissues of the body.[2,106] The most dangerous effect of IL-1β secretion is the exacerbation of the damage during any chronic disease and acute tissue injury in cancer and COVID-19, to list a few. Thus, the release mechanisms of IL-1β represent a therapeutic target. Consequently, cytokine secretion, in particular IL-1β, has a huge impact on host well-being. Therefore, understanding the secretory pathways of IL-1β is critical in understanding inflammation, inflammation-related diseases, and resistance to pathogens. However, the mechanism of IL-1β release has proven to be elusive. It does not follow the conventional ER Golgi route of secretion. The important questions of how this protein is exported from cells and how its control affects the inflammatory response remain unanswered. This is partially due to the lack of tools that could allow, in a high-throughput manner, the monitoring, visualization, and manipulation of the interleukin pathways. Understanding long-lasting modifications requires tracking and control of the dynamics of regulatory processes, revealing the mechanism of the inflammatory response and how it resists pathogens. For example, this would require the determination of how a specific secretory pathway leads to enhanced cellular and tissue damage in chronic or acute diseases; how to control it; and when the inflammation begins.

To ensure real-time tracking (monitoring), one may first develop special light sources operating in visible and near-infrared wavelengths and then use these light sources to illuminate a NP torch (nanotorch) and collect its response; and next, to internalize the nanotorch into a biological emulator macrophage and inspect it with super-resolution visualization tools.

6.2. PH-Controlled Nanodrug Delivery Across Central Nervous System Barriers

A unique characteristic of the central nervous system (CNS) is the existence of physical barriers that keep the microenvironment of the brain and spinal cord in a narrow homeostatic range. Among three barriers—blood–brain (BBB), blood–cerebrospinal fluid (CSF), and arachnoid—the BBB is composed of endothelial cells that are connected by tight junctions and regulate the transport of molecules between the circulatory system and the brain.[116] Yet, while intactness of the BBB is essential for normal brain function, it stands as an obstacle to the permeation of many medicines targeted for the treatment of brain diseases such as tumors.[117] The retina in the eye is an integral part of the CNS, and its blood supply is similar to that of the brain and spinal cord. Indeed, the proper function of the retina requires strict regulation over the molecular composition of the extracellular environment to ensure normal function of the neuronal elements. As an extension of the BBB, the endothelium of the retinal microvessels is interconnected by tight junctions and forms the blood–retinal barrier (BRB).[118] However, while the brain is protected by the skull and direct access requires surgical intervention, the retina of the eye allows direct visualization. The fact that they share similar properties has increased, in recent years, the idea of the "eye, a window to brain," that is, imaging and detection of ocular (retina) abnormalities for diagnosis and monitoring of neurodegenerative diseases.[119–123] Inversely, several ocular pathologies such as glaucoma,[124] age-related macular degeneration,[125] and diabetic retinopathy (DR)[126] present characteristics of neurodegenerative disorders, including microvascular injury, neuroinflammation, and atrophy, that are associated with visual deficits and blindness.[127] DR, for example, is a
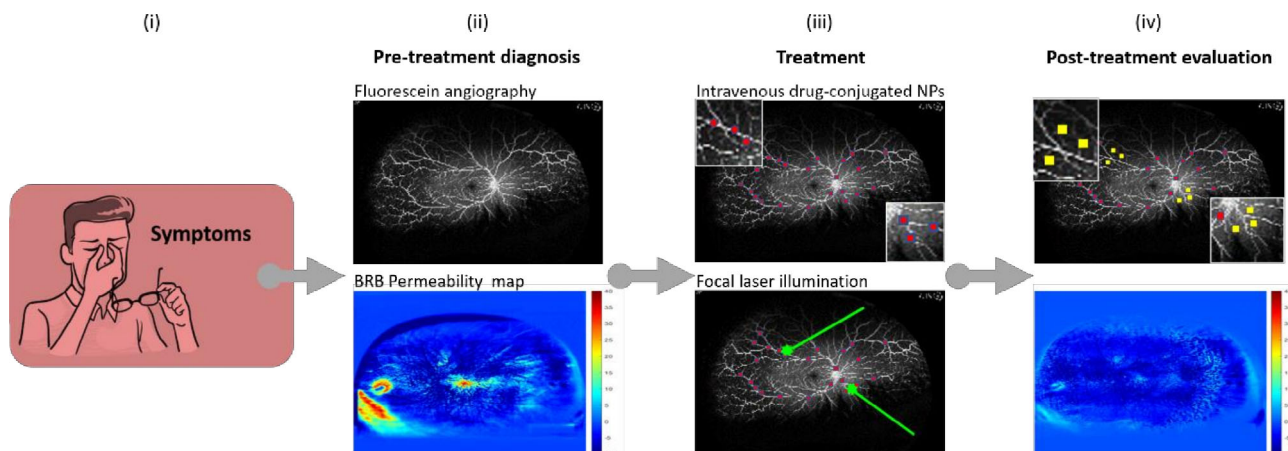
Figure 9. i) A patient with early-stage visual problems and suspected RD will be ii) referred for fluorescein angiography examination, followed by algorithm-based image analysis for detection of BRB leakiness (pretreatment). iii) The patient will be injected intravenously with anti-VEGF-conjugated NPs (red spots), followed by focal laser illumination over areas diagnosed with intact BRB to enhance drug delivery (treatment). iv) Illumination-induced drug NP extravasation (yellow spots, PH) will result in effective retinal therapy.

**ADVANCED
SCIENCE NEWS**

www.advancedsciencenews.com

**ADVANCED
PHOTONICS
RESEARCH**

www.adpr-journal.com

specific complication of diabetes mellitus and is the leading cause of blindness in adults. In DR, hypoxia-associated vascular injury leads to excess production of the vascular endothelial growth factor (VEGF), which further induces abnormal neovascularization and increases the risk to BRB dysfunction and bleeding. Therefore, in recent years, the first-line therapy to DR is the administration of anti-VEGF antibodies. However, like BBB, BRB limits the penetration of antibodies into the retina and forces direct intraocular injection, a process that is invasive, expensive, and associated with significant complications.[128] The nanojet (PH), as described earlier, generates the optomechanical force that allows the motion of NPs. Thus, focal laser illumination of retinal microvessels following noninvasive systemic administration (e.g., intravenous) of VEGF antibodies-conjugated NPs has the potential to push the NP complexes across the BRB, that is, from the blood into the retina. If this drug delivery approach works, it will allow a noninvasive and efficient treatment for DR.

7. Summary and Future Remarks

Despite efforts and advances in engineering light-activated tools for optical visualization at the single-cell level that we overview in this article, a general and robust methodology for investigating and controlling cellular functions by the use of light remains elusive due to fundamental deficits in current methods. These deficits arise from several flaws stemming from current research tools, specifically the nature of 1) optical microscopy; 2) fluorescence microscopy; 3) super-resolution radial fluctuations; and 4) optical tweezers. By merging forces into a multidisciplinary research approach for developing light-activated tools, it may become possible to mitigate biological processes such as the inflammatory reaction; to prevent cellular death necrosis in a wide range of diseases such as COVID-19-caused pneumonia, cancer, and autoimmune diseases; and to establish new experiments for cellular processes still to be discovered (**Figure 9**).

Ultimately, light-based techniques may enable the development of a toolbox for the study of secretory pathways of any protein or biomaterial by the use of light and to generate a novel paradigm for expanding the complexity of function that can be imparted to biological systems by leveraging and integrating research in electro-optics, engineering, nanotechnology, and biology.

Acknowledgements

Conflict of Interest

The authors declare no conflict of interest.

Keywords

blood–brain barrier, immunology, optical forces, single cells tracking interleukin

[1] A. Katiyi, J. Zorea, A. Halstuch, M. Elkabets, A. Karabchevsky, *Biosens. Bioelectron.* **2020**, *161*, 112240.

[2] M. Monteleone, A. C. Stanley, K. W. Chen, D. L. Brown, J. S. Bezbradica, J. B. von Pein, C. L. Holley, D. Boucher, M. R. Shakespear, R. Kapetanovic, V. Rolfes, M. J. Sweet, J. L. Stow, K. Schroder, *Cell Rep.* **2018**, *24*, 1425.

[3] E. Hecht, *Optics fourth edition*, 5ed., Pearson Education India, Addison Wesley, **2002**.

[4] I. Abdulhalim, A. Karabchevsky, C. Patzig, B. Rauschenbach, B. Fuhrmann, E. Eltzov, R. Marks, J. Xu, F. Zhang, A. Lakhtakia, *Appl. Phys. Lett.* **2009**, *94*, 063106.

[5] A. Karabchevsky, I. Abdulhalim II, C. Khare, B. Rauschenbach, *J. Nanophotonics* **2012**, *6*, 061508.

[6] Z. Bao, S. Wang, W. Shi, S. Dong, H. Ma, *J. Proteome Res.* **2007**, *6*, 3835.

[7] W. E. Moerner, M. Orrit, *Science* **1999**, *283*, 1670.

[8] X. Li, H. Ma, L. Nie, M. Sun, S. Xiong, *Anal. Chim. Acta* **2004**, *515*, 255.

[9] M. Nirmal, B. O. Dabbousi, M. G. Bawendi, J. Macklin, J. Trautman, T. Harris, L. E. Brus, *Nature* **1996**, *383*, 802.

[10] S. Culley, K. L. Tosheva, P. M. Pereira, R. Henriques, *Int. J. Biochem. Cell Biol.* **2018**, *101*, 74.

[11] C. Eggeling, K. I. Willig, S. J. Sahl, S. W. Hell, *Q. Rev. Biophys.* **2015**, *48*, 178.

[12] L. Schermelleh, A. Ferrand, T. Huser, C. Eggeling, M. Sauer, O. Biehlmaier, G. P. Drummen, *Nat. Cell Biol.* **2019**, *21*, 72.

[13] E. Wegel, A. Göhler, B. C. Lagerholm, A. Wainman, S. Uphoff, R. Kaufmann, I. M. Dobbie, *Sci. Rep.* **2016**, *6*, 1.

[14] E. Betzig, G. H. Patterson, R. Sougrat, O. W. Lindwasser, S. Olenych, J. S. Bonifacino, M. W. Davidson, J. Lippincott-Schwartz, H. F. Hess, *Science* **2006**, *313*, 1642.

[15] S. T. Hess, T. P. Girirajan, M. D. Mason, *Biophys. J.* **2006**, *91*, 4258.

[16] J. S. Biteen, M. A. Thompson, N. K. Tselentis, G. R. Bowman, L. Shapiro, W. Moerner, *Nat. Methods* **2008**, *5*, 947.

[17] M. J. Rust, M. Bates, X. Zhuang, *Nat. Methods* **2006**, *3*, 793.

[18] J. P. Pezacki, J. A. Blake, D. C. Danielson, D. C. Kennedy, R. K. Lyn, R. Singaravelu, *Nat. Chem. Biol.* **2011**, *7*, 137.

[19] Y. Park, C. Depeursinge, G. Popescu, *Nat. Photonics* **2018**, *12*, 578.

[20] G. Popescu, *Quantitative Phase Imaging of Cells and Tissues*, McGraw-Hill Education, New York **2011**.

[21] A. Ashkin, J. M. Dziedzic, T. Yamane, *Nature* **1987**, *330*, 769.

[22] A. Ashkin, J. M. Dziedzic, *Science* **1987**, *235*, 1517.

[23] A. Grigorenko, N. Roberts, M. Dickinson, Y. Zhang, *Nat. Photonics* **2008**, *2*, 365.

[24] A. Heifetz, S.-C. Kong, A. V. Sahakian, A. Taflove, V. Backman, *J. Comput. Theor. Nanosci.* **2009**, *6*, 1979.

[25] L. Yue, B. Yan, Z. Wang, *Opt. Lett.* **2016**, *41*, 1336.

[26] A. Kovrov, A. Novitsky, A. Karabchevsky, A. S. Shalin, *Ann. Phy.* **2018**, *530*, 1800129.

[27] J. Y. Lee, B. H. Hong, W. Y. Kim, S. K. Min, Y. Kim, M. V. Jouravlev, R. Bose, K. S. Kim, I.-C. Hwang, L. J. Kaufman, C. W. Wong, P. Kim, K. S. Kim, *Nature* **2009**, *460*, 498.

[28] Z. Wang, W. Guo, L. Li, B. Luk'yanchuk, A. Khan, Z. Liu, Z. Chen, M. Hong, *Nat. Commun.* **2011**, *2*, 1.

[29] H. Yang, R. Trouillon, G. Huszka, M. A. Gijs, *Nano Lett.* **2016**, *16*, 4862.

[30] Y. Li, X. Liu, B. Li, *Light: Sci. Appl.* **2019**, *8*, 1.

[31] A. Darafsheh, G. F. Walsh, L. Dal Negro, V. N. Astratov, *Appl. Phys. Lett.* **2012**, *101*, 141128.

[32] Y. Geinz, A. Zemlyanov, E. Panina, *Russ. Phys. J.* **2015**, *57*, 9.

[33] A. Ashkin, *Phys. Rev. Lett.* **1978**, *40*, 729.

[34] D. Gao, W. Ding, M. Nieto-Vesperinas, X. Ding, M. Rahman, T. Zhang, C. Lim, C.-W. Qiu, *Light: Sci. Appl.* **2017**, *6*, 17039.

[35] A. A. R. Neves, C. L. Cesar, arXiv preprint arXiv:1902.04807, **2019**.

[36] C. Bradac, *Adv. Opt. Mater.* **2018**, *6*, 1800005.

[37] A. Ashkin, *Proc. Natl. Acad. Sci.* **1997**, *94*, 4853.

[38] R.-J. Essiambre, *Proc. Natl. Acad. Sci.* **2021**, *118*, 7.

[39] I. Minin, Y. E. Geints, A. Zemlyanov, O. Minin, *Opt. Express* **2020**, *28*, 22690.

[40] J. P. Barton, D. R. Alexander, S. A. Schaub, *Journal of Applied Physics* **1989**, *66*, 4594.

[41] L. Novotny, B. Hecht, *Principles of Nano-Optics*, Cambridge University Press, UK **2006**.

[42] J. Chen, J. Ng, Z. Lin, C. T. Chan, *Nat. Photonics* **2011**, *5*, 531.

[43] B. T. Draine, *Astrophys. J.* **1988**, *333*, 848.

[44] R. Grimm, M. Weidemüller, Y. B. Ovchinnikov, *Adv. At. Mol. Opt. Phys.* **2000**, *42*, 95.

[45] J. E. Baker, R. P. Badman, M. D. Wang, *WIREs Nanomed. Nanobiotechnol.* Wiley Online Library, **2018**, *10*, e1477.

[46] A. S. Ang, I. V. Minin, O. V. Minin, S. V. Sukhov, A. S. Shalin, A. Karabchevsky, in *META 2018, the 9th Int. Conf. on Metamaterials, Photonic Crystals and Plasmonics*, France, **2018**, p. 2.

[47] J. C. Maxwell, *A Treatise on Electricity and Magnetism*, Clarendon Press, Oxford **1873**.

[48] P. Lebedev, *Ann. Phys.* **1901**, *311*, 433.

[49] E. F. Nichols, G. F. Hull, *Phys. Rev.* **1901**, *13*, 307.

[50] P. Lebedev, *Astrophys. J.* **1910**, *31*, 385.

[51] A. Ashkin, *Phys. Rev. Lett.* **1970**, *24*, 156.

[52] A. Ashkin, J. M. Dziedzic, J. E. Bjorkholm, S. Chu, *Opt. Lett.* **1986**, *11*, 288.

[53] A. Dogariu, S. Sukhov, J. Sáenz, *Nat. Photonics* **2013**, *7*, 24.

[54] S. Sukhov, A. Dogariu, *Rep. Prog. Phys.* IOP Publishing, **2017**, *80*, 112001.

[55] I. Minin, O. Minin, Y. E. Geints, E. Panina, A. Karabchevsky, *Atmos. Oceanic Opt.* **2020**, *33*, 464.

[56] L. P. Neukirch, E. Von Haartman, J. M. Rosenholm, A. N. Vamivakas, *Nat. Photonics* **2015**, *9*, 653.

[57] C.-Y. Liu, F.-C. Lin, *Opt. Commun.* **2016**, *380*, 287.

[58] S. Lecler, S. Perrin, A. Leong-Hoi, P. Montgomery, *Sci. Rep.* **2019**, *9*, 1.

[59] I. V. Minin, O. V. Minin, C.-Y. Liu, H.-D. Wei, Y. E. Geints, A. Karabchevsky, *Opt. Lett.* **2020**, *45*, 4899.

[60] M. Spector, A. S. Ang, O. V. Minin, I. V. Minin, A. Karabchevsky, *Nanoscale Adv.* **2020**, *2*, 2595.

[61] A. S. Ang, S. V. Sukhov, A. Dogariu, A. S. Shalin, in *Progress in Electromagnetics Research Symp.*, St. Petersburg, Russia **2017**.

[62] S. Lecler, Y. Takakura, P. Meyrueis, *Opt. Lett.* **2005**, *30*, 2641.

[63] A. Darafsheh, *J. Phys.: Photonics* **2021**, *3*, 022001.

[64] S. Wang, T. Ding, *Nanoscale* **2019**, *11*, 9593.

[65] B. S. Luk'yanchuk, R. Paniagua-Domínguez, I. V. Minin, O. V. Minin, Z. Wang, *Opt. Mater. Express* **2017**, *7*, 1820.

[66] A. Heifetz, J. J. Simpson, S.-C. Kong, A. Taflove, V. Backman, *Opt. Express* **2007**, *15*, 17334.

[67] Z. Chen, A. Taflove, V. Backman, *Opt. Express* **2004**, *12*, 1214.

[68] L. Zhao, C. K. Ong, *J. Appl. Phys.* **2009**, *105*, 123512.

[69] A. S. Ang, I. V. Minin, O. V. Minin, S. V. Sukhov, A. Shalin, A. Karabchevsky, in *Proc. of the the 9th Int. conf. on Metamaterials, Photonic crystals and Plasmonics*, Marseille, France, June **2018**.

[70] M. Spector, A. S. Ang, O. V. Minin, I. V. Minin, A. Karabchevsky, *Nanoscale Adv.* **2020**, *2*, 5312.

[71] X. Cui, D. Erni, C. Hafner, *Opt. Express* **2008**, *16*, 13560.

[72] Y. Li, H. Xin, X. Liu, Y. Zhang, H. Lei, B. Li, *ACS Nano* **2016**, *10*, 5800.

[73] C. B. Schaffer, A. Brodeur, E. Mazur, *Meas. Sci. Technol.* **2001**, *12*, 1784.

[74] A. K. De, D. Roy, A. Dutta, D. Goswami, *Appl. Opt.* **2009**, *48*, G33.

[75] L. Yue, O. V. Minin, Z. Wang, J. N. Monks, A. S. Shalin, I. V. Minin, *Opt. Lett.* **2018**, *43*, 771.

[76] I. V. Minin, O. V. Minin, *SpringerBriefs in Physics*, Springer International Publishing, Cham, **2016**.

[77] A. S. Ang, A. Karabchevsky, I. V. Minin, O. V. Minin, S. V. Sukhov, A. S. Shalin, *Sci. Rep.* **2018**, *8*, 1.

[78] I. V. Minin, O. V. Minin, G. M. Katyba, N. V. Chernomyrdin, V. N. Kurlov, K. I. Zaytsev, L. Yue, Z. Wang, D. Christodoulides, *Appl. Phys. Lett.* **2019**, *114*, 031105.

[79] K. Dholakia, G. D. Bruce, *Nat. Photonics* **2019**, *13*, 229.

[80] G. Gu, L. Shao, J. Song, J. Qu, K. Zheng, X. Shen, Z. Peng, J. Hu, X. Chen, M. Chen, Q. Wu, *Opt. Express* **2019**, *27*, 37771.

[81] Y. Zhang, C. Min, X. Dou, X. Wang, H. P. Urbach, M. G. Somekh, X. Yuan, *Light: Sci. Appl.* **2021**, *10*, 1.

[82] L. Kaufman, T. Cooper, G. Wallace, D. Hawke, D. Betts, D. Hess, F. Lagugné-Labarthet, in *Plasmonics In Biology And Medicine XVI*, vol. *10894*, International Society for Optics and Photonics, Bellingham, WA **2019**, p. 108940B.

[83] A. Karabchevsky, A. Mosayyebi, A. V. Kavokin, *Light: Sci. Appl.* **2016**, *5*, 16164.

[84] D. R. Dadadzhanov, I. A. Gladskikh, M. A. Baranov, T. A. Vartanyan, A. Karabchevsky, *Sens. Actuators B: Chem.* **2021**, *333*, 129453.

[85] D. P. Cherney, J. C. Conboy, J. M. Harris, *Anal. Chem.* **2003**, *75*, 6621.

[86] I. Prada, L. Amin, R. Furlan, G. Legname, C. Verderio, D. Cojoc, *BioTechniques* **2016**, *60*, 1.

[87] M. S. Friddin, G. Bolognesi, A. Salehi-Reyhani, O. Ces, Y. Elani, *Commun. Chem.* **2019**, *2*, 1.

[88] J. Burkhartsmeyer, Y. Wang, K. S. Wong, R. Gordon, *Appl. Sci.* **2020**, *10*, 394.

[89] H. Wang, X. Wu, D. Shen, *Opt. Lett.* **2016**, *41*, 1652.

[90] M. P. MacDonald, G. C. Spalding, K. Dholakia, *Nature* **2003**, *426*, 421.

[91] A. Keloth, O. Anderson, D. Risbridger, L. Paterson, *Micromachines* **2018**, *9*, 434.

[92] R. Weissleder, *Nat. Biotechnol.* **2001**, *19*, 316.

[93] A. Kusumi, Y. Sako, *Curr. Opin. Cell Biol.* **1996**, *8*, 566.

[94] M. Li, T. Lohmuller, J. Feldmann, *Nano Lett.* **2015**, *15*, 770.

[95] F. Tian, J. Conde, C. Bao, Y. Chen, J. Curtin, D. Cui, *Biomaterials* **2016**, *106*, 87.

[96] H. Yuan, S. Khatua, P. Zijlstra, M. Yorulmaz, M. Orrit, *Angew. Chem.* **2013**, *125*, 1255.

[97] D. R. Dadadzhanov, T. A. Vartanyan, A. Karabchevsky, *Nanomaterials* **2020**, *10*, 1265.

[98] A. Karabchevsky, A. Katiyi, A. S. Ang, A. Hazan, *Nanophotonics* **2020**, *9*, 3733.

[99] D. R. Dadadzhanov, T. A. Vartanyan, A. Karabchevsky, *Opt. Express* **2019**, *27*, 29471.

[100] Z. Wang, N. Joseph, L. Li, B. Luk'Yanchuk, *Proc. Inst. Mech. Eng., Part C: J. Mech. Eng. Sci.* **2010**, *224*, 1113.

[101] M. S. Dhoni, W. Ji, *J. Phys. Chem. C* **2011**, *115*, 20359.

[102] K. Yee, *IEEE Transactions on antennas and propagation*, IEEE, **1996**, *14*, 302.

[103] T. Weiland, *Int. J. Numer. Modell. Electron. Networks Devices Fields* **1996**, *9*, 295.

[104] A. Taflove, S. C. Hagness, M. Piket-May, *Computational Electrodynamics: The Finite-Difference Time-Domain Method* **2005**, p. 3.

[105] W. P. Carpes Jr., L. Pichon, A. Razek, *Int. J. Numer. Modell. Electron. Networks Devices Fields* **2000**, *13*, 527.

[106] R. Sitia, A. Rubartelli, *Biol. Chem.* **2020**, *295*, 7799.

[107] J. Kim, H. Y. Gee, M. G. Lee, *J. Cell Sci.* **2018**, *131*, 12.

[108] S. Debaisieux, F. Rayne, H. Yezid, B. Beaumelle, *Traffic* **2012**, *13*, 355.

[109] T. G. Santos, V. R. Martins, G. N. M. Hajj, *Int. J. Mol. Sci.* **2017**, *18*, 946.

[110] M. E. Woodbury, T. Ikezu, *J. Neuroimmune Pharmacol.* **2014**, *9*, 92.

[111] A. Rubartelli, F. Cozzolino, M. Talio, R. Sitia, *EMBO J.* **1990**, *9*, 1503.

[112] G. Lopez-Castejon, D. Brough, *Cytokine Growth Factor Rev.* **2011**, *22*, 189.

[113] S. L. Cassel, F. S. Sutterwala, *Eur. J. Immunol.* **2010**, *40*, 607.

[114] K. Schroder, J. Tschopp, *Cell* **2010**, *140*, 821.

[115] M. S. Boyles, T. Kristl, A. Andosch, M. Zimmermann, N. Tran, E. Casals, M. Himly, V. Puntes, C. G. Huber, U. Lütz-Meindl, A. Duschl, *J. Nanobiotechnol.* **2015**, *13*, 1.

[116] N. J. Abbott, L. Rönnbäck, E. Hansson, *Nat. Rev. Neurosci.* **2006**, *7*, 41.

[117] C. D. Arvanitis, G. B. Ferraro, R. K. Jain, *Nat. Rev. Cancer* **2020**, *20*, 26.

[118] A. Naylor, A. Hopkins, N. Hudson, M. Campbell, *Int. J. Mol. Sci.* **2020**, *21*, 211.

[119] N. Cheung, T. Mosley, A. Islam, R. Kawasaki, A. R. Sharrett, R. Klein, L. H. Coker, D. S. Knopman, D. K. Shibata, D. Catellier, T. Y. Wong, *Brain* **2010**, *133*, 1987.

[120] M. Koronyo-Hamaoui, Y. Koronyo, A. V. Ljubimov, C. A. Miller, M. K. Ko, K. L. Black, M. Schwartz, D. L. Farkas, *Neuroimage* **2011**, *54*, S204.

[121] M. M. Moschos, G. Tagaris, L. Markopoulos, L. Margetis, S. Tsapakis, M. Kanakis, C. Koutsandrea, *Eur. J. Ophthalmol.* **2011**, *21*, 24.

[122] M. L. Monteiro, D. B. Fernandes, S. L. Apóstolos-Pereira, D. Callegaro, *Invest. Ophthalmol. Visual Sci.* **2012**, *53*, 3959.

[123] A. London, I. Benhar, M. Schwartz, *Nat. Rev. Neurol.* **2013**, *9*, 44.

[124] N. Gupta, Y. H. Yücel, *Curr. Opin. Ophthalmol.* **2007**, *18*, 110.

[125] T. Yoshida, K. Ohno-Matsui, S. Ichinose, T. Sato, N. Iwata, T. C. Saido, T. Hisatomi, M. Mochizuki, I. Morita, *J. Clin. Invest.* **2005**, *115*, 2793.

[126] R. Simó, C. Hernández, European Consortium for the Early Treatment of Diabetic Retinopathy (EUROCONDOR, *Br. J. Ophthalmol.* **2012**, *96*, 1285.

[127] J. M. Sivak, *Invest. Ophthalmol. Visual Sci.* **2013**, *54*, 871.

[128] K. G. Falavarjani, Q. Nguyen, *Eye* **2013**, *27*, 787.

[129] Y.-C. Li, H.-B. Xin, H.-X. Lei, L.-L. Liu, Y.-Z. Li, Y. Zhang, B.-J. Li, *Light: Sci. Appl.* **2016**, *5*, 16176.

Alina Karabchevsky is an assistant professor at the School of Electrical and Computer Engineering at Ben-Gurion University of the Negev (BGU) and the Chair of IEEE Women in Engineering Affinity Group (Israel Section). She is the head of the Light-on-a-Chip Center at the BGU. Her main research interests lie in the areas of integrated photonics and microfibers, all-dielectric photonics, plasmonics, microfluidics, and optomechanics.

Tal Elbaz obtained her B.Sc. in chemical engineering from the Ben-Gurion University in 2016. In 2019, Tal joined the Electrooptics and Photonics Engineering Department at Ben-Gurion University as an M.Sc. student under the supervision of Dr. Karabchevsky and is expected to graduate in 2021. Her main interests lie in the areas of optomechanics.

Aviad Katiyi obtained his B.Sc. in electrooptical engineering from the Lev Institute of Jerusalem in 2013. In 2017 and 2021, Aviad obtained his M.Sc. and Ph.D., respectively, in photonics and electro-optics engineering at Ben-Gurion University under the supervision of Dr. Karabchevsky. His main interests lie in the areas of guided-wave optics.

Ofer Prager is a young research associate in the BBB Lab in the Faculty of Health Sciences and a member of the Zlotowski Center for Neuroscience at the Ben-Gurion University of the Negev. Ofer is a graduate of the Department of Biotechnology Engineering and finished his doctoral studies in the Department of Physiology and Cell Biology at Ben-Gurion University. He studies in rodents neurovascular coupling under physiological and pathological conditions and the role of hypertension in brain pathologies.
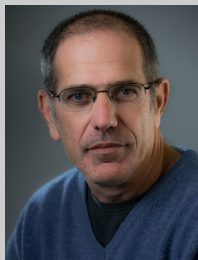
Alon Friedman is a professor of neuroscience and Dennis Chair in Epilepsy Research at Dalhousie University in Halifax and a professor in the Department Brain and Cognitive Sciences, at Ben-Gurion University of Negev in Israel. He completed his medical and doctoral training at Ben-Gurion University and did his residency training in neurosurgery at Soroka University Medical Center in Israel. He did his postdoctoral training at the Charitè Medical University in Berlin, Germany, as an Alexander von-Humboldt fellow.